Accepted Manuscript

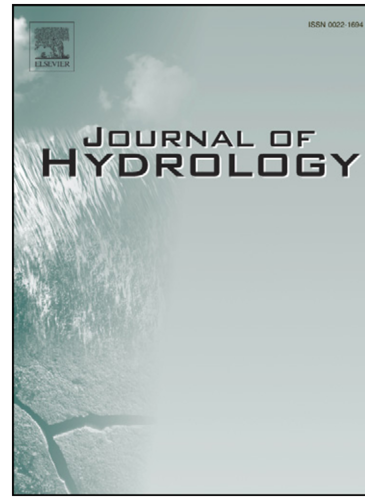

Calibration of Satellite Measurements of River Discharge Using a Global Hydrology Model

G. Robert Brakenridge, Sagy Cohen, Albert J. Kettner, Tom De Groeve, Son V. Nghiem, James P.M. Syvitski, Balazs M. Fekete

PII: S0022-1694(12)00838-4
DOI: http://dx.doi.org/10.1016/j.jhydrol.2012.09.035
Reference: HYDROL 18487

To appear in: *Journal of Hydrology*

Received Date: 3 March 2012
Revised Date: 7 September 2012
Accepted Date: 15 September 2012

Calibration of Satellite Measurements of River Discharge Using a Global Hydrology Model

Manuscript submitted for publication March 3, 2012

G. Robert Brakenridge[1], Sagy Cohen[1,2], Albert J. Kettner[1], Tom De Groeve[3], Son V. Nghiem[4], James P.M. Syvitski[1], and Balazs M. Fekete[5]

[1]Community Surface Dynamics Modeling System, Institute of Arctic and Alpine Research, University of Colorado, Boulder, Colorado 80309, USA

[2]Department of Geography, University of Alabama, Box 870322, Tuscaloosa, AL 35487, USA

[3]Joint Research Centre, European Commission, Ispra, Italy

[4]Jet Propulsion Laboratory, California Institute of Technology Pasadena, California, 91109, USA

[5]CUNY Environmental CrossRoads Initiative, NOAA-CREST Center, The City College of New York, City University of New York, New York, New York, 10031, USA

Email contact corresponding author: Robert.Brakenridge@Colorado.edu

Keywords: rivers, water discharge, runoff, remote sensing, hydrological model, Water Balance Model

Abstract

Measurements of river discharge and watershed runoff are essential to water resources management, efficient hydropower generation, accurate flood prediction and control, and improved understanding of the global water cycle. Previous work demonstrates that orbital remote sensing can measure river discharge variation in a manner closely analogous to its measurement at ground stations, and using reach flow surface area instead of stage as the discharge estimator. For international measurements, hydrological modeling can, in principle, be used to provide the needed calibration of sensor data to discharge. The present study tests this approach and investigates the accuracy of the results. We analyze 6 sites within the U.S. where gauging station, satellite measurements, and WBM model results are all available. Knowledge is thereby gained concerning how accurately satellite sensors can measure discharge, if the signal is calibrated only from global modeling results without any ground-based information. The calibration (rating) equations obtained for the remote sensing signal are similar, whether based on gauging station or on model information: r^2 correlation coefficients for least squares fits at one example site (#524; White River, Indiana) are both .66 (n = 144, comparing monthly daily maxima, minima, and mean, 2003-2006). Space-based 4-day mean discharge values for this site when using the model calibration are accurate to within +/- 67% on the average (n = 1824; largest percent errors occur at low discharges), and annual total runoff is accurate to +/- 9 %, 2003-2008. Comparison of gauging station versus modeled discharge commonly indicates a small positive model bias; the observed errors of satellite-observed annual runoff are also positive and could be improved by bias removal from the rating curves. Also, analysis of a large flood event, along the Indus River in 2010, shows that the model does not capture flood wave attenuation by overbank flow, and thus predicts faster flood wave celerity and higher peak discharge than was measured by the remote sensing. The incorporation of overbank processes would improve discharge estimation via modeling, and also facilitate more accurate satellite-based measurement of peak discharge. The analysis shows that existing and planned microwave sensors can usefully characterize global river discharge dynamics, and that water balance model-based rating curves provide acceptable calibration of remote sensing signal to discharge.

1. Introduction

Measurements of river discharge and watershed runoff are essential to water resources management, efficient hydropower generation, accurate flood prediction and control, and improved understanding of the global water cycle. River discharge at-a-site is an integrated signal of water cycle processes over the catchment area upstream, and large amounts of variability over relatively small amounts of time commonly occur. This makes high frequency (daily) measurements necessary for many rivers (Fekete et al., 2012). Major efforts have been made to improve the international availability of ground-based discharge data, but many nations do not share hydrological data, and the network of ground stations on a global basis is inadequate. Rivers and tributary streams transgress political borders, causing downstream nations to experience severe constraints in predicting surface water incoming from upstream. Global hydrological modeling can assist in evaluating runoff (Littlewood et al., 2003; Sivapalan et al., 2003); such modeling is complementary to direct measurements, but not an accurate substitute for them (e.g. Cohen et al., 2011).

Space-based observational approaches for direct, sustained characterization of river discharge and runoff have so far been little utilized. Yet, they are now feasible, using existing and planned sensors. New processing techniques using frequent-revisit microwave-frequency sensing (Brakenridge et al., 2007) have demonstrated a capability to track discharge changes via the sensitive response to water surface area changes. Such information can be obtained globally and in “near real time” (within several hours after satellite overpass). These data require some method of calibration to discharge to be most useful. Here we employ a global water balance runoff model (WBM; Wisser et al., 2010; Wisser et al., 2008) to calibrate remote sensing to discharge: at measurement sites within the U.S. that are coincident to comparison ground gaging stations. Error analysis indicates that model-based calibration of the remote sensing signal can substitute for calibration by ground-based discharge data at many sites without significant loss of discharge accuracy. However, along some major rivers (the study example is the Indus, in Pakistan), WBM does not presently account for very significant flood wave attenuation via overbank flooding. Peak discharge downstream is thus over-estimated, and model improvements would facilitate more accurate rating curves.

2. Measuring Discharge and Runoff From Space

Previous work demonstrates that orbital remote sensing from a variety of sensors has the capability to characterize river discharge variation in a manner closely analogous to its measurement at ground stations (Brakenridge et al., 2005; Brakenridge et al., 2007; Khan et al., 2011; Smith, 1997; Smith et al., 1996; Temimi, 2011). Thus, for ground gauging stations, frequent or continuous river stage heights are calibrated to discharge using infrequent, current meter traverses. These intermittent ("actual discharge") measurements obtained in the field sample flow velocities and channel cross sectional areas under varying flow conditions, as stage values are recorded. Empirical, "rating curves" that compare stage to discharge are thereby developed. Conventional ground-based discharge values based on stage-discharge rating curves have an accuracy of 5 to 10% (Hirsch and Costa, 2004; Olson and Norris, 2007; Rantz et al. 1982; Schmidt, 2003).

In comparison, and for measurement via orbital remote sensing methods, consider the flow continuity equation:

$$Q = wdu \qquad (1)$$

where Q is discharge in m^3/sec, w is flow width (m), d is flow depth (m), and u is flow velocity (m/sec). Inherent to flow continuity is that measurements which monitor flow width also provide a proxy indicator of changing discharge (unless the channel banks are vertical). Along most rivers, w is similar to d in its sensitivity to discharge change (Bjerklie et al., 2004); both are more robust predictors of discharge than u. Thus, w measurements can be transformed, via a rating curve, to actual discharge, if calibration estimates of actual high, medium, and low discharges can be obtained while sustained width-sensitive observation is underway (Smith, 1997; Brakenridge et al., 2007).

As is the case for gauging stations on the ground, the local river and floodplain channel geometry control the accuracy of rating curve relations in a satellite-based approach. For stage-based measurements at gauging stations, a desirable site exhibits stable channel geometry with relatively permanent and steep channel banks, where discharge changes are accommodated mainly by changes in d and stage. For observation via satellite, w changes can be most frequently observed, and a desirable measurement site is one where discharge changes are accommodated mainly by changes in w. Most river systems exhibit reaches of both types. Some rivers are in fact difficult to monitor by gauging stations due to variable channel geometry, meandering or braiding channels, and other dynamic processes. Remote sensing responsive to *w*, (or, for a defined reach, flow area) offers a potentially better approach at such locations.

In this regard, there are actually two alternatives for sensing changes in river "width": 1) measurement of actual flow width changes, at individual cross sections (Bjerklie et al., 2003), or 2) remote sensing signal measurements that are sensitive to flow area change, along a defined measurement reach (Smith, 1997). Monitoring water surface area is particularly attractive, because it takes advantage of the spatial coverage provided by remote sensing. Reach surface water area is also less prone to local variation in riverbed geometry, due to accomodating the net effects of local scour and fill. In contrast, measuring flow width is observationally demanding, because of the dual challenge of high spatial resolution and frequent sampling in time. Furthermore, high-resolution characterizations of a river at specific cross sections would require frequent recalibration due to seasonal, annual, and inter-annual changes in riverbed, location, and meandering patterns (just as stage rating curves do). This paper employs the second approach, which is most appropriate for remote sensing from above: using sensors that are sensitive to flow area change, have frequent revisit characteristics, and with sufficiently high spatial resolution to record small flow area changes.

River discharge can also be modeled instead of observed: by parameterization of catchment areas and measurement of forcing variables, including precipitation. This independent approach offers an opportunity to calibrate the remote sensing to discharge values. Through modeling, if changing catchment precipitation, soil moisture, evapotranspiration, and other upstream watershed characteristics can be measured or constrained, reasonably accurate discharge can be estimated and for potentially unlimited locations along a river. As daily precipitation and other data fields are ingested, updated model-based discharge estimates can be calculated at the same time intervals. Contemporary watershed runoff modeling uses advanced computational capabilities to scale flow routing and other functions to relatively fine scale watershed characterizations (e.g. to a global grid at approximately 10 km).

This paper considers whether global hydrology model-based discharge information can provide the needed calibration of remote sensing observations. Such capability would enable sustained satellite characterization of river discharge via either flow area or (from altimetry) stage, and where *in situ* data are unavailable. We analyze a suite of 6 river measurement sites within the U.S. where surface gauging station, remote sensing, and model results are co-located. First , the temporal sampling needed to adequately characterize river flow variation is considered. Next we describe the passive microwave remote sensing that provides the needed measurements. In order to test ground-based versus model-based calibration outcomes, we employ the WBM water balance model (Wisser et al., 2010; Wisser et al., 2008) and obtain predicted daily discharges for the measurement sites. Rating equations for the remote sensing signal are developed and compared via two different methods: 1) using modeled discharge values, and 2) using ground station-measured discharge. The co-location with gauging stations also allows constraints to be placed on the accuracy of satellite-based discharge measurements using either approach.

3. Temporal Sampling for Discharge Characterization

Earth-observing satellites are currently being planned to help measure global river discharge and water storage changes and constrain runoff modeling (Alsdorf et al., 2003; Alsdorf et al., 2007; Durand et al., 2008; Durand et al., 2010). Potential remote sensing revisit frequencies for any given river location vary widely: from hourly, for geostationary satellites, to ~ weekly, for low latitude locations in the proposed Surface Water and Oceans Topography (SWOT) mission (Biancamaria et al., 2010). Because of the constellation of sensors planned or already available, there are clear opportunities for complementary measurements, in which more-precise but relatively infrequent observational data from experimental missions are combined, when available, with less precise but ongoing and frequent surveillance of rivers by operational systems.

The minimum temporal sampling needed to adequately characterize river flow varies with river flow regime. Along some very large rivers, where the daily discharge is strongly auto-correlated and the rate of change is not fast, sampling frequency requirements may not be high. As a result, except during major flooding, surface stations that provide a daily record may actually oversample. However, water discharge for most rivers is a rapidly varying flux, at least during part of a season (Shiklomanov et al., 2006). Thus: 1) a 10-fold discharge change may occur along many rivers over a period of only several days, or less, and 2) a large proportion of total annual river runoff may be concentrated in flood seasons lasting only several weeks to several months. Also, measuring low flow during a sustained drought, or high flow during a flood, requires sustained high frequency observation:

the duration of extreme flow in days is as important as high precision individual measurements in obtaining total monthly runoff. Shiklomanov et al (2006), analyzing Arctic rivers, describe in detail this strong dependence on sampling frequency in measuring accurate values for even total annual runoff.

Although stage-discharge rating curves exhibit various errors, including hysteresis (Dottori et al., 2009), transformation of frequently or continuously measured stage to estimate discharge has long been accomplished within acceptable and well-constrained accuracy and precision. An inherent motivation of this overall approach is close-interval sampling in time. In some cases (e.g. flood hydrographs along smaller rivers), the time scale may be hours, but the large proportion of ground station-based river discharge data is reported using daily time intervals. An important challenge for remote sensing of river discharge is to achieve at least this same frequent sampling in time while progressively improving, with better sensors and processing techniques, the accuracy of individual (daily) measurements.

4. Passive Microwave Radiometry for River Discharge Measurement

One reason for utilizing microwave information is that, at selected frequencies, microwave radiation suffers relatively little interference from cloud cover. Also, night overpasses can be utilized; the signal does not require solar illumination. These attributes allow for frequent data retrievals on a global basis (e.g. pixel spatial resolutions of ~10km, daily or near-daily repeats).

Factors that affect total upwelling microwave brightness from a mixed water and land surface measured by a single image pixel include: a) sensor calibration characteristics (stability of its signal through time), b) perturbation of the signal by land surface changes (e.g., surface temperature, soil moisture, crop changes, snowfall, and rainfall), and c) contrast between land and water at the frequency being used (very different values of emissivity for water and land favor the most sensitive monitoring of water area change). Also, microwave frequencies have more commonly been used to observe soil moisture changes (Schmugge, 1980; Theis et al., 1982; Ulaby et al., 1978; Wang et al., 1982; Wang et al., 1980; Njoku et al., 2003; Nghiem et al., 2012). Because of the sensitivity of microwave emission to soil moisture as well as surface water, measurements of surface water change must incorporate some method to remove variations caused by temporal changes in soil moisture.

The fundamental basis of passive microwave sensitivity to river discharge for mixed water/land pixels was analyzed with a microwave emission model derived from first principles (Brakenridge et al., 2007). The emission model is developed from fluctuation-dissipation theory, incorporating the non-isothermal conditions of riverine environments. Correlations of electromagnetic fields derived from Maxwell's equations with different signal polarizations can be cast in form of a hyperbolic cotangent factor of the quantum energy ($\hbar\omega$) over the absolute physical temperature (Tsang et al., 1985), operated on a tensor product involving the polarization vector, complex effective permittivity, and dyadic Green's function (Nghiem et al., 1990).

A difficulty in interpreting the microwave radiance measured by a satellite is that it is a product of both physical temperature and emissivity. Whereas the emissivity contains water information, the physical temperature can change quickly, depending on time of the day, solar shading (e.g., topographic shadowing), and weather conditions. Whereas many passive microwave methods use the polarization ratio (PR) and the frequency gradient ratio (GR) to cancel physical temperature within a pixel, PR and GR also reduce the sensitivity to water change (Brakenridge et al., 2007). The key for river discharge measurement is to cancel the physical temperature, also using a ratio approach, but with the river measurement pixel amplitude value compared to nearby but separate calibration pixel values. This approach retains a high sensitivity to river discharge variability expressed as water surface area changes (Brakenridge et al., 2007).

Finally, the reach water surface area rather than flow width approach also greatly relaxes the spatial resolution requirements for sensing flow variation. The microwave signal from a defined river reach, and geographically including both: a) lower channel water area, and b) upper channel bar surfaces and floodplain dry land, will track discharge: as the river rises and falls, the reach water and land proportion changes, and only a sensitive numeric indicator of such is needed. An actual map of water versus land is not required. The microwave signal variation from individual, relatively large (~ 10 km) pixels centered over rivers can thus be used directly: the measured reach is one such pixel (Brakenridge et al., 2007). This approach in fact requires relatively large image pixels, because it is important that the highest floods not completely fill or saturate a pixel. The sensitivity, noise characteristics, and stability of the remote sensing signal are, however, critical, and the remote sensing data must be accompanied by high quality geocoding: any variation in the actual ground surface being sampled by repeat measurements introduces noise.

5. Geographic Sampling Considerations for Global Measurements

For global characterization of freshwater runoff through rivers, a large array of sites, at least several thousand, is needed: this still provides only several hundred per continent and leaves many major streams and rivers un-monitored. There are many potential issues involved with efficient design of gauging station networks sampling global scale land areas. For example, although a set of relatively few gauges located near the mouths of large rivers can capture a considerable portion of the total discharge to oceans (Fekete et al., 2002), the remaining contributing landmasses are fragmented into hundreds of small watersheds. Also, discharge should best be measured just downstream of the confluences of tributaries, because discharge varies downstream only gradually along trunk streams, whereas tributaries typically add a large sudden increment that is important to capture.

Design criteria for global sampling schemes are beyond the scope of this paper. However, previous MODIS imaging of global surface water variability (Brakenridge et al., 2005; Brakenridge and Kettner, 2012) provides abundant (n= 2583) suitable locations where flow area variation has already been measured optically on an intermittent basis (Figure 1). At these locations, it has been demonstrated that a water area-sensitive remote sensing signal will monitor flow variability. These potential measurement sites are thus a useful starting point in designing a global array.

Microwave signal data for these and additional sites (De Groeve, 2010; De Groeve et al., 2006; De Groeve and Riva, 2009; Kugler and De Groeve, 2007) added more recently are available at: http://www.gdacs.org/flooddetection/. The sensitivity of each measurement site to discharge variation, and the character of each site's signal-to-discharge rating curve, are both a function of individual site characteristics, and especially channel and floodplain morphology. An efficient calibration approach is needed to convert these numerous discharge-sensitive records to discharge units.

6. Choice of Data and Processing Strategies

The data available to monitor rivers in the microwave domain includes the 37 GHz channel provided by the SMMR (Scanning Multichannel Microwave Radiometer) in1978-1987, the SSM/I (Special Sensor Microwave Imager) aboard the Defense Meteorological Satellite Program satellite series (1987 to present), the 37 GHz channel aboard TRMM (Tropical Rainfall Measurement Mission, 1998 to present), similar frequency but including V/H polarimetric data provided by AMSR-E, (Advanced Microwave Scanning Radiometer for Earth Observation System) July, 1, 2002-October 4, 2011, and the recently launched (early 2012) AMSR instrument aboard the Japanese satellite GCOM-w. Most data from these sensors are made available in swath image formats (not geolocated into map projections, but with accompanying latitude and longitude coordinate information for each pixel) and also as geocorrected raster images (pixels of fixed dimensions and geographic location within global or large-region raster files).

In this study, we describe two passive microwave *data sources* and also two *signal processing methods*. However, the comparisons use mainly one data source and one method: AMSR-E data processed according to the first method, below. It was used prior to transition to the second method in the current processing scheme.

Method 1 uses AMSR-E 36.5 GHz, horizontal H polarization, descending orbit (night) data, as obtained by a swath image pixel value retrieval algorithm (De Groeve et al., 2006). In this algorithm, data from within a 5 km radius of a geographic point target are retrieved, as determined by the geolocation information for each pixel (the values obtained are from pixels whose centers are within that radius). The river measurement reaches (the "M" data) are, therefore, circular in shape. Also, information from a fixed and nearby (dry land) comparison site (the "C" data) is retrieved from the same swath image and includes an area of identical size, manually selected to be free from mapped streams and rivers. M/C, a dimensionless ratio value, is the discharge estimator; as noted, use of the ratio isolates any change that affects only one of the pixels and, in particular, river flow area variation. Data processed in this way show a strong correlation to measured discharge at many sites in the U.S. (Figure 2A, Figure 3).

Method 2 uses AMSR-E 36.5 GHz, total amplitude (V and H polarizations combined), and including data from both ascending and descending orbits, as mosaicked within georeferenced, global-coverage, near real time raster images. These image data are in latitude and longitude (Plate Carree) projection, with pixel dimensions of .0833 degrees (approximately 9.27 km square at the equator but with decreasing east-west km dimensions at increasing distances from the equator).

The processing, as automatically performed by the Global Flood Detection System in Ispra, Italy (De Groeve, 2010; De Groeve and Riva, 2009), also calculates a dimensionless ratio value from these rasters, but the comparison value is based on the brightest (driest) values from a 7 x 7 pixel array in the raster and centered on the measurement pixel. The measurement pixels each contain the same latitude and longitude point targets as for the first method, but the fixed pixel ground footprint means that the river reach being sampled differs significantly (with a maximum shift of a half pixel size, or about 5 km). This approach does not require the manual selection of the calibration pixel, making it computable anywhere in the world. Its other advantage is that single-pixel variation in the calibration information cannot so strongly affect the discharge-estimator signal. In detail, the algorithm calculates the (95th percentile) brightest value of the calibration pixels and the ratio of that value to the measurement pixel value (Figure 2B, Figure 3). Previous comparisons of the two methods for other sites indicate the results to be strongly correlated (Figure 2) and to exhibit comparable amounts of scatter and error (De Groeve and Riva, 2009).

In both processing methods, a 4-day forward running mean is applied, because AMSR-E does not provide daily revisits at lower latitudes. Instead, some locations commonly are revisited every two days, or, very rarely, only every three days, as the AMSR-E orbit precesses. The 4-day running mean facilitates a most-current update, daily, with values for every location globally. In any comparisons to ground station data or model output, therefore, we also use 4 day running mean data. Future microwave sensors such as NASA's planned GPM mission will provide more-than-daily revisits and thus a daily update without multi-day averaging will be possible at all latitudes.

The AMSR-E data offer the capability to consistently monitor river measurement sites for nearly a decade (data begin in July, 2002) and for ground footprints of approximately 10 km; however, the sensor ceased operation on October 4, 2011. The 37 GHz frequency and H polarization were selected in method 1 because H polarization data exhibits the strongest differential response to water and land (Brakenridge et al., 2007) at this frequency and with lesser sensitivity to soil moisture. The ongoing TRMM satellite output provides similar microwave data (but from a non-polar orbit, and without high latitude coverage). The signal processing at GDACS/GFDS is presently using these TRMM data; as noted, the methods described are also applicable to an array of similar frequency remote sensing from other sensors.

7. The WBM global hydrology model

The WBM model includes the water balance/transport model first introduced by (Vörösmarty et al., 1998; Vörösmarty et al., 1989) and subsequently modified (Wisser et al., 2010; Wisser et al., 2008). WBM is a relatively simple but robust water budgeting scheme that takes into account climate forcings (air temperature and precipitation in its simplest form) and estimates various water stocks (soil moisture and groundwater) and fluxes (evapotranspiration, surface runoff, groundwater recharge and baseflow). WBM has been applied successfully in small watersheds at 200m spatial resolution, up to a global scale at 6 minute grid (approximately 11 km at the equator) cell sizes. WBM was probably the first hydrological model applied to a global domain. The main difference between WBM and comparable large-scale hydrological models is the high degree of flexibility in specifying computation domains and input data and configuration. WBM has demonstrated a bias of 5-8mm/yr (Fekete et al., 2002; Vörösmarty et al., 1998) with respect to annual runoff (297mm/yr). Numerous studies have shown that the most critical input variable is precipitation (Fekete et al.,2004; Biemans et al. 2009).

At its core, the surface water balance of non-irrigated areas is a simple soil moisture budget expressed as:

$$dW_s / dt = \begin{cases} -g(W_s)\left(E_p - P_a\right) & P_a \le E_p \\ P_a - E_p & E_p < P_a \le D_{WS} \\ D_{WS} - E_p & D_{ws} < P_a \end{cases} \qquad (2)$$

driven by $g(W_s)$, a unitless soil function:

$$g\left(W_s\right) = \frac{1 - e^{\left(-\alpha \frac{W_s}{W_c}\right)}}{1 - e^{-\alpha}} \qquad (3)$$

W_s is the soil moisture, E_p is the potential evapotranspiration, P_a is the precipitation (rainfall P_r combined with snowmelt M_s), and D_{ws} is the soil moisture deficit: the difference between available water capacity W_c, which is a soil and vegetation dependent variable (specified externally) and the soil moisture. The unit-less empirical constant α is set to 5.0 following Vörösmarty et al. (1989).

Flow routing from grid to grid cell follows the downstream grid cell tree topology (which only allows conjunctions of grid cells upstream, without splitting to form islands or river deltas) and is implemented using the Muskingum-Cunge equation, which is a semi implicit finite difference scheme to the diffusive wave solution to the St. Venant equations (ignoring the two acceleration terms in the momentum equation). The equation is expressed as a linear combination of the input flow from current and previous time step ($Q_{in\ t-1}$, $Q_{in\ t}$) and the released water from the river segment in the previous time step ($Q_{out\ t-1}$) to calculate new grid-cell outflow:

$$Q_{out\ t} = c_1\, Q_{in\ t} + c_2\, Q_{in\ t-1} + c_3\, Q_{out\ t-1} \qquad (4)$$

As described by Wisser et al., 2010), the Muskingum coefficients ($c_1\ c_2\ c_3$) are estimated from channel properties (width, depth, slope, and length) using the relations of Cunge (1969) and Dooge et al. (1982). We use a power function approximation of channel geometry $w = a\, y^b$ to express the relationship between the width (w) and depth; b dictates the ratio and of flood-wave celerity to flow velocity.

In this paper, the WBM water discharge predictions are from a daily, global scale simulation at 6 arc-minute (~11 km) spatial resolution. Daily predictions are averaged by a 4 day running mean window to align with the satellite microwave 4 day averaging process. The precipitation dataset is from the Global Precipitation Climate Center GPCC, Offenbach, Germany (gpcc.dwd.de) using their “Full” product, which combines long-term precipitation climatology, derived from the entire data archive, with anomalies estimated from the operating meteorological stations at any given time. The GPCC “Full” product is available at monthly time steps at 30 arc-minute spatial resolution. Daily partitioning of the monthly precipitation totals was established by computing the daily fraction of the monthly precipitation from the NCEP reanalysis product (Kalnay et al., 1996; Kistler et al., 2001). A six minute topological network (Vörösmarty, Fekete, Meybeck, & Lammers, 2000) was derived from the high resolution gridded network HydroSHEDS using SRTM elevation data set (Lehner, Verdin, & Jarvis, 2008). A comprehensive list of the model input datasets is provided (Cohen et al., 2011).

8. Testing WBM Model Output For Rating Curve Generation

The United States is monitored by a relatively dense array of operational hydrological gaging stations. Data from these allow us to evaluate the effectiveness of a model-based approach to calibrate remote sensing measurements to discharge values.

We chose 6 sites for satellite-based measurement in the continental U.S. (Figure 4) that are coincident to or in very close proximity with *in situ* stations providing daily measurements between 2002-2010. The site locations and attributes represent diverse geomorphological, land-use and climate settings (Table 1). Although this is a small number of sites, their analysis provides the opportunity to consider in detail the relationship of the remote sensing to station-observed discharge variation and that provided by the model.

For each site, the empirical relation (the rating curve) between the remote sensing signal and ground station-measured water discharge is constructed. As well, the signal is compared to coeval model results, to produce a separate and independent model-based rating curve for each site. This would be one method for calibrating thousands of river measurement sites distributed globally (Figure 1). By comparing the rating curves, and the resulting discharge time series, we can investigate how accurately satellite sensors can measure discharge, *if the signal is calibrated only from global modeling results*: without any ground-based information.

Three temporally coincident datasets are used in each case (Figure 5):

1. Daily, including the complete (9 year) daily values (n = 3285);
2. Monthly, including the monthly mean, maximum and minimum daily values for 12 months (n = 36);
3. Yearly, including the annual mean, maximum and minimum daily values (n =27).

For consistency, second-order polynomial rating curves are used to evaluate the scatter plots created in all cases (Table 2). We compared our results using other regression equations without substantial change in the results. Because of relatively large scatter at the lower end of some river discharge regimes (the flow area method becomes less sensitive once flow is fully confined within the lower channel), there is an additional requirement that all portions of the polynomial curve remain monotonic or flat.

We seek also to determine the optimal calibration strategy (daily, monthly or yearly values) that could be applied to a large number of sites. Figure 6 shows daily water discharge time-series (2002-2010) for the six sites and as based on both model-based and station-measured calibrations. The plots also include the measured discharge at the co-located gaging station (Figure 4 and Table 1) for comparison. The top plot for each site is obtained from the daily data rating curve; the middle from calibration with monthly statistics; and the bottom from yearly statistics (e.g., figures 5a, 5b and 5c respectively). Black lines in Figure 6 show the ground station-measured discharge; blue lines the satellite results based on using ground station data for the rating curves, and red lines the satellite results which use model output for the rating curves.

Overall, visual comparison of the remote sensing signal to station-measured discharge yields a generally strong time series correlation. Figure 4 also provides such comparison on an expanded temporal scale; the applicable Nash-Sutcliffe values are .60 and .61. In the Figure 6 plots, however, we are concerned with understanding how the choice of calibration, via rating curves, affects the discharge results. Calculating the Nash-Sutcliffe descriptive statistic assists in this regard: higher values should indicate more correlated results (without further consideration of other factors bearing on such statistics, including autocorrelation, time lags, data distributions, influence of outliers, etc).

From Figure 6, discharge estimation based on daily data calibration (rating curves such as in Figure 5a) is similar to that obtained when the rating curve uses monthly and yearly statistics: if station data rather than modeling are used for the rating curve. Nash-Sutcliffe values range among the sites between .11-.37 (satellite-observed, compared to gauging station data). In contrast, discharge values obtained from model-based calibration methods (dashed orange lines in Figure 6) can vary depending on whether daily versus yearly or monthly data are used for the rating curves, and also there is more variability by site: the modeling, as expected, is more accurate at some sites than at others.

In this regard, modeled daily data-based rating equations predict lower than observed discharge (most clearly in site #530; Figure 6). Comparison of WBM model results to measured discharge further indicates that the model itself generally under-predicts mean discharge (Table 1). In sites #997 and #2483, the daily data-based rating curve produces more accurate results than monthly and yearly calibrations (e.g., for #997, Nash-Sutcliffe values of .2 for the daily-based calibration compare to -1.0 for the monthly and yearly). In these two cases, WBM considerably over-predicted high discharge events (Figure 6).

The results overall demonstrate the sensitivity of any model-based calibration approach to the accuracy of the model predictions. They indicate that using yearly and monthly statistics to calibrate the AMSR-E signal data to discharge, in most cases, better constrains the size of very high discharge events: even though, for some events, there is over-estimation of the flood magnitude (i.e. sites 997 and 2483; Figure 6). WBM Model-based calibration, in general, is found to be a viable approach for translating the remote sensing signal to discharge, and we find no major advantage in using daily information rather than monthly or yearly mean, maximum, and minimum values, as defined above, and within this analyzed 9 year period of record.

To further evaluate errors associated with the method 2 data and associated processing, daily station-measured and remote sensing-measured values (n = 1824) were obtained for one site (#524), 2003-2006 using the model-based, monthly value-based rating curve. Assuming the gauging station data as representing true discharge, the average error departure of the remote sensing (daily-incremented) discharge values is 67%, with percentage errors being largest at times of low flow. These relatively large daily value errors are reduced in the calculation of runoff totals from these data, and in part because high error values at low flows less strongly affect runoff totals. For annual values 2003-2008, the average error is 9%.

Previous work (Brakenridge et al., 2007) indicates one source of error in the daily values produced by this remote sensing technique is the lack of exact temporal match between station and remote sensing discharge series. For example, major flood peak discharge as measured by surface gauging stations may precede by 1-2 days the peak recorded by remote sensing (which is measuring reach flow area along an entire river measurement site). Such lags produce a negative departure (remote sensing value – station value) as the peak flow passes the station and while the reach area is progressively flooding. Then, several days later, a positive error occurs as stage is already declining at the station (in part due to the overbank flow). Thus, the peak discharge value may be recorded accurately by both ground-based stage and satellite-based flow area techniques, but the timing may differ and lead to large increases in the average daily measurement error and in descriptive statistics such as the Nash-Sutcliffe coefficient.

9. Modeling and Remote Measurement of an Extreme Flood

As noted, for many locations globally, daily discharge information from surface gauging stations is difficult or impossible to obtain. Even where gauging station data are available and are public, large floods can temporarily damage or entirely disable surface stations. Although orbital remote sensing can, presently, provide valuable river discharge information and monthly and annual runoff volumes, there are significant errors still to be addressed (examine the time series shown in figures 3 and 6). Perhaps the greatest asset of the remote sensing capability here detailed is its ability to be quickly and easily applied to new measurement sites of interest, without field access. An example is now presented to enable further examination of the utility of satellite microwave river discharge measurements in general, and those based on WBM model calibration in particular. The results further emphasize that accurate remote sensing measurement via this approach will depend on the quality of any hydrological model used for calibration.

During the summer monsoon of 2010, The upstream Khyber-Pakhtunkhwa region of Pakistan experienced rainfall totals >300 mm July 27-30, and the Punjab, Gilgit Baltistan and Azad Kashmir provinces received July rainfall totals of >500 mm. The trunk stream (Indus) flood hydrograph then traversed 500 km of river reach to the sea, mainly along a meandering channel that is constrained within a 15 to 20 km wide floodplain by engineered artificial levees. All of this floodplain (and more) was inundated (Syvitski and Brakenridge, submitted manuscript).

Analysis of optical remote sensing data indicates that most damage was caused by multiple failures of irrigation system levees, and by barrage-related backwater effects that initiated failures and led to avulsions (sudden changes in flow location). We consider here the difference between the modeled and the remotely-observed flood hydrograph at an illustrative remote sensing measurement site.

The WBM-modeled peak discharge for this flood at site #2010, south of a major levee failure and partial avulsion of the Indus at the Tori Bund, is ~26,000 m^3/sec, with flow being elevated above 15,000 m^3/sec for only several days (Figure 7). However, the model includes no limitations on the volume of water transported in a river at a point in time (no change to overbank flow conditions is incorporated). This can cause over-prediction of the magnitude of high flow events (as shown in the U.S. sites #997 and #2483; see also Cohen et al., 2011). Also, the modeled water is transported much too rapidly downstream. A new version of WBM (currently in testing) will address these limitations by incorporating an over-bank flow component that acknowledges the reality of channel overtopping during large discharges. Also, the present model does not include the possibility of avulsion.

Comparison of the remotely sensed discharge at station #2009, upstream of the avulsion at Tori, and at #2010 indicate a reduction of measured peak flow downstream of the breach by ~10,000 m3/sec (Syvitski and Brakenridge, submitted manuscript). Figure 7 shows the very different shape of the observed hydrograph at this site compared to that modeled for it. Thus, avulsion reduced the peak flow, and, also, the flood was experienced for much longer (22 days of > 15,000 m^3/sec) than the model predicted. During large floods, and even along heavily engineered rivers, major attenuation of the flood wave typically occurs, and this is illustrated in the Indus example. This attenuation can be measured in detail by this form of remote sensing. However, its adequate characterization by modeling at this spatial scale remains an important task for future work. The lack of accurate modeled peak discharge for extreme events may in turn generally affect model-based rating curves and the remote sensing-assessment of peak discharge magnitudes.

10. Conclusion

The results indicate that microwave satellite discharge characterization at selected river reaches can approach *in-situ* ground station information in its utility for several applications, including the analysis of flood dynamics and the quantification of longer term watershed runoff volumes. However, remote sensing of rivers through these methods does require some form of calibration to discharge values via rating equations. The examples we analyzed indicate that the needed transformation of water-area sensitive remote sensing to river discharge can be accomplished by incorporation of global runoff model results. Using the described or similar microwave data and processing approaches, and for river measurement sites whose channel and floodplain morphologies favor flow area variability, 4-day running mean daily discharges as measured via satellite compare favorably with information obtained by gauging stations. The timing and duration of periods of high and low flow are accurately constrained, and the relative magnitude in m^3/sec of flood peaks can be determined. However, daily value accuracies exhibit significant errors, in part due to a lack of exact temporal match in the timing of some major flood peaks. For annual runoff expressed in mm/yr, observed errors, at the suite of sites examined, and using a global model-based calibration approach was relatively small. This suggests that the measurement technology is already able to deliver significant new information for water balance studies at many international locations, and without support by ground-based information.

We stress the synergy between different remote sensing approaches for discharge measurement. One upcoming space agency mission (the U.S./France SWOT satellite) is being designed to provide global data sets of accurate swath radar altimetry-based river stage and slope, but without a long-term record and with a short (3-year) nominal mission life. Flow area measurements through existing and planned microwave sensors can, meanwhile, be made frequently (~ daily); they can potentially be extended back about three decades in time at favorable sites, and they can be continued while SWOT is collecting data and afterwards. Several satellites are currently providing appropriate, stable, well-calibrated, water area-sensitive data; these can already be used. For many research efforts and well as practical applications, both long-term data and current near-real-time observations are necessary. The challenge is to develop processing methodologies that can ingest, process, and disseminate the results, provide reliable error estimates, and allow synergistic incorporation of new sensor data when such become available.

In regard to the best calibration/rating curve approaches, our analysis indicates significant variation in the rating curve equations, depending on whether model-based daily, monthly or yearly statistics are used. In general, daily data-based rating curves do not always accurately estimate the highest flow events: polynomial or other regressions applied to the comparisons of modeled and observed daily data from the calibration period may not accurately capture the relation between the largest discharge and the remote sensing signal, and especially when the modeled routing of flood waves inadequately captures overbank and other flow attenuation processes. Rating curves based instead on monthly or yearly maximum and minimum statistics better characterize the signal/discharge relation at the extremes. Preliminary work using the method 2 data and processing indicates that incorporating a 5 year period of record for both modeled and observed values, and using monthly daily maxima, minima, and mean values (n =180) commonly produces rating curves with monotonic, second order polynomial least square regression r^2 values >.6 at favorable sites, and also provides the most accurate prediction of peak flow values.

11. Acknowledgments

Part of the research (by Nghiem) was carried out at the Jet Propulsion Laboratory, California Institute of Technology, under a contract with the National Aeronautics and Space Administration. The other authors thank as well the U.S. National Science Foundation, the European Commission, and NASA for support, and the Universit of Colorado, Community Surface Dynamics Modeling System (CSDMS) for computing time on high-performance computing clusters.

11. References

Alsdorf, D., D., Lettenmaier, Vorosmarty, C.J., 2003. The need for global, satellite-based observations of terrestrial surface waters. AGU EOS Transactions, 84(269): 274-276.

Alsdorf, D., Rodriguez, E., Lettenmaier, D.P., 2007. Measuring surface water from space. Rev. Geophys, Res. Lett., 45: 1-24.

Biancamaria, S. et al., 2010. Preliminary characterization of SWOT hydrology error budget and global capabilities,. IEEE J. Sel. Top. Appl., 3: 6-19.

Bjerklie, D.M., Dingman, S.L., Vorosmarty, C.J., Bolster, C.H., Congalton, R.G., 2003. Evaluating the potential for measuring river discharge from space. Journal of Hydrology, 278: 17-38.

Bjerklie, D.M., Moller, D.K., Smith, L.C., Dingman, S.L., 2004. Estimating discharge in rivers using remotely sensed hydraulic information. Journal of Hydrology, 309: 191-209.

Brakenridge, G.R., Anderson, E., Nghiem, S.V., Chien, S., 2005. Space-based measurement of river runoff. EOS, Transactions of the American Geophysical Union, v. 86, no. 19, p. 185-188.

Brakenridge, G.R., Kettner, A.J., 2012. The Surface Water Record, Version 2, http://floodobservatory.colorado.edu/Tech.html.

Brakenridge, G.R., Nghiem, S.V., Anderson, E., Mic, R., 2007. Orbital microwave measurement of river discharge and ice status. Water Resources Research, 43(W04405, doi:10.1029/2006WR005238).

Cohen, S., Kettner, A.J., Syvitski, J.P.M., 2011. WBMsed: a distributed global-scale riverine sediment flux model - model description and validation. Computers and Geosciences, doi: 10.1016/j.cageo.2011.08.011.

De Groeve, T., 2010. Flood monitoring and mapping using passive microwave remote sensing in Namibia. Geomatics, Natural Hazards and Risk, 1(DOI:10.1080/19475701003648085): 19-35.

De Groeve, T., Kugler, Z., Brakenridge, G.R., 2006. Near Real Time Flood Alerting for the Global Disaster Alert and Coordination System. Proceedings ISCRAM2007 (B. Van de Walle, P. Burghardt and C.Nieuwenhuis, eds.): 33-39.

De Groeve, T., Riva, P., 2009. Early flood detection and mapping for humanitarian response. Proceedings of the 6th International ISCRAM Conference – Gothenburg, Sweden, May 2009 J. Landgren, U. Nulden and B. Van de Walle, eds.: 1-13.

Dottori, F., Martina, M.L.V., Todini, E., 2009. A dynamic rating curve approach to indirect discharge measurement. Hydrol. Earth. Syst. Sci, Discuss., 6: 859-896.

Durand, M., K. et al., 2008. Estimation of bathymetric depth and slope from data assimilation of swath altimetry into a hydrodynamic model. Geophys. Res. Lett, 35(L20401): doi:10.1029/2008GL034150.

Durand, M., Rodríguez, E., Alsdorf, D.E., Trigg, M., 2010. Estimating river depth from remote sensing swath interferometry measurements of river height, slope, and width IEEE Journal of selected topics in applied Earth observations and remote sensing, 3(1): 20-31.

Fekete, B.M., Looser, U., Pietroniro, A., Robarts, R., 2012. Discharge is best monitored on the ground. Journal of Hydrometeorology, in press.

Fekete, B.M., Vörösmarty, C.J., Grabs, W., 2002. High Resolution Fields of Global Runoff Combining Observed River Discharge and Simulated Water Balances. Global Biochemical Cycles, 16(15): 1-6.

Fekete, B.M., Vörösmarty, C.J., Roads, J., Willmott, C., 2004. Uncertainties in precipitation and their impacts on runoff estimates. Journal of Climatology, 17: 294-303.

Hirsch, R.M., Costa, J.E., 2004. U.S. stream flow measurement and data dissemination improve. EOS, Transactions of the American Geophysical Union, v. 85, no. 21, p. 197,203.

Khan, S.I. et al., 2011. Satellite remote sensing and hydrological modeling for flood inundation mapping in Lake Victoria Basin: Implications for hydrologic prediction in ungauged basins. IEEE Transactions on Geoscience and Remote Sensing, 49(doi: 10.1109/TGRS.2010.205751): 85-95.

Kugler, Z., De Groeve, T., 2007. The Global Flood Detection System. EUR 23303 EN, Luxembourg: Office for Official Publications of the European Communities: 45.

Littlewood, I.G., Croke, B.F.W., Jakeman, A.J., Sivapalan, M., 2003. The role of "top-down" modelling for prediction in ungauged basins. Hydrological Processes, 17(8): 1673-1679.

Nghiem, S.V., Borgeaud, M., Kong, J.A., Shin, R.T., 1990. Polarimetric remote sensing of geophysical media with layer random medium model, Progress in Electromagnetics Research. Elsevier, New York, pp. 1-73.

Nghiem, S.V, Wardlow, D.B., Allured, D., Svoboda, M.D., LeComte, D., Rosencrans, M., Chan, K.S., Neumann, G., 2012. Microwave remote sensing of soil moisture – Science and applications, Chapter 9, Part III, in Remote Sensing of Drought – Innovative Monitoring Approaches, Drought and Water Crises Book Series, Taylor and Francis, ISBN 978-1-4398-3557-9, pp. 197-226.

Njoku, E.G., Jackson, T.J., Lakshmi, V., Chan, T.K., Nghiem, S.V., 2003. Soil moisture retrieval from AMSR-E, IEEE Trans. Geosci. Remote Sens., 41(2): 215-229.

Olson, S.A., and Norris, J.M., 2007, U.S. Geological Survey streamgaging . . . from the National Streamflow Information Program: U.S. Geological Survey Fact Sheet 2005–3131, 4 p.

Rantz, S.E., others, a., 1982. Measurement and computation of streamflow: volume 1, measurement of stage and discharge. U.S. Geological Survey Water Supply Paper 2175.

Schmidt, A.R., 2002. Analysis of stage-discharge relations for open-channel flows and their associated uncertainties. Ph.D. Dissertation, University of Illinois at Urbana-Champaign.

Schmugge, T.J., 1980. Microwave approaches in hydrology. Photogramm. Eng. Remote Sens., 46: 495-507.

Shiklomanov, A.I. et al., 2006. Cold region river discharge uncertainty—estimates from large Russian rivers. Journal of Hydrology, 326: 231-256.

Sivapalan, M. et al., 2003. IAHS Decade on Predictions in Ungauged Basins (PUB), 2003-2012: Shaping an exciting future for the hydrological sciences. Hydrological Sciences Journal, 48(6): 857-880.

Smith, L.C., 1997. Satellite remote sensing of river inundation area, stage, and discharge: A review. Hydrological Processes, 11: 1427-1439.

Smith, L.C., Isacks, B.L., Bloom, A.L., Murray, A.B., 1996. Estimation of discharge from three braided rivers using synthetic aperture radar satellite imagery. Water Resources Research, 32(7): 2021-2034.

Syvitski, J.P.M., Brakenridge, G.R., 2012. Causation and avoidance of catastrophic flooding along the Indus River, Pakistan. In Review.

Temimi, M., 2011. A multi-temporal analysis of AMSR-E data for flood and discharge monitoring during the 2008 flood in Iowa. Hydrological Processes, 25: 2623–2634.

Theis, S.W., McFarland, M.J., Rosenthal, W.D., Jones, C.L., 1982. Microwave remote sensing of soil moistures. RSC-3458-129, Remote Sensing Center, Texas A&M University, College Station, TX.

Ulaby, F.T., Batlivala, P.P., Dobson, M.C., 1978. Microwave backscatter dependence on surface roughness, soil moisture, and soil texture: Part I - bare soil. IEEE Trans. Geosci. Elec., GE-16: 286-295.

Vörösmarty, C.J., Federer, C.A., Schloss, A.L., 1998. Potential evaporation functions compared on US watersheds: Possible implications for global-scale water balance and terrestrial ecosystem modeling. Journal of Hydrology, 207: 147-169.

Vörösmarty, C.J. et al., 1989. Continental scale models of water balance and fluvial transport: An application to South America. Global Biochemical Cycles, 3: 241-265.

Wang, J., O'Neill, P., Engman, E., al., e., 1982. Remote measurements of soil moisture by microwave radiometers at BARC test site II. 83954, NASA.

Wang, J.R., Shiue, J.C., McMurtrey, J.E., 1980. Microwave remote sensing of soil moisture content over bare and vegetative fields. Geophys. Res. Lett., 7: 801-804.

Wisser, D., Fekete, B.M., Vörösmarty, C.J., Schumann, A.H., 2010. Reconstructing 20th century global hydrography: a contribution to the Global Terrestrial Network- Hydrology (GTN-H). Hydrology and Earth System Sciences, 14(1): 1-24.

Wisser, D. et al., 2008. Global irrigation water demand: Variability and uncertainties arising rom agricultural and climate data sets. Geophysical Research Letters, 35(doi:10.1029/2008GL035296).

Figure Captions

Figure 1. Satellite river measurement sites (n = 2583) where optical remote sensing (2001-2010) detects significant surface water area variation within the site reaches (10 km in length). Near-daily time series of passive microwave signal have been obtained and archived for each site since July 1, 2002. Evaluation of the 10 yr+ time series allows the daily signal data to be binned into low flow (yellow dots, <5th percentile of complete series), normal flow (blue dots), moderate flood (purple dots, recurrence interval > 1.33 yr via Log Pearson III) and large flood (bright red dots, > 5 yr recurrence via Log Pearson III). Red dots at high latitudes are processing errors due to ice-covered conditions.

Figure 2. A (top), Plot of the microwave discharge estimator ratio, 4-day running means, calculated according to method 1, for each day, January 1, 2009-December 31, 2010, versus 4-day forward running mean gauging station discharge, White River, southern Indiana (remote sensing site 524; gauging station USGS 03360500 White River at Newberry, Indiana). B (bottom), Plot of the estimator ratio, calculated according to method 2, versus the gauging station information, same time period. Vertical scales are in ft^3/sec.

Figure 3. A, top: satellite-estimated daily 4-day running mean river discharge, site 524, in red, compared to 4-day running mean discharge measured at the co-located gauging station (blue). Rating curve was based on comparison of daily station and (method 2) satellite data; applicable Nash-Sutcliffe statistic is .60. B, bottom: satellite-estimated discharge, red, using a rating based on the WBM model-produced discharge information (same remote sensing data); applicable Nash-Sutcliffe statistic is .61. The model-based rating curve underestimates peak discharge but characterizes average flow conditions quite accurately. Vertical scales are in ft^3/sec.

Figure 4. Location map for the remote sensing river measurement sites and co-located USGS gaging stations.

Figure 5. Example plots (site #925) of method 1 microwave discharge estimator values versus WBM-simulated discharge. A, top: Daily values using the entire dataset. B, middle: Monthly values (monthly mean, minima and maxima). C, bottom: Yearly values, using only yearly mean, minimum and maximum. The daily value-based rating equation underestimates flood flows.

Figure 6. Nine year (2002-2010) daily time series of water discharge for the 6 remote-sensing sites (numbering corresponds to Figure 4 and Table 1). Gauging station-measured discharge is plotted with a thick black line, microwave signal-estimated discharge based on the gauging station data is plotted with a blue line, and microwave signal-estimated discharge based on WBM model-predicted discharge is plotted with a dashed orange line.

The top plot for each site is for calibration using the entire daily dataset, the middle plot is for calibration using only the monthly statistics and the bottom plot for calibration using only yearly statistics.

Figure 7. Time series for the year 2010 showing the time lag between WBM-simulated and microwave-observed discharge (dashed black and solid blue lines respectively) at site #2010 on the Indus River, Hala, Pakistan. Modeling predicts an earlier and higher flood crest, and more rapid dissipation than was observed via remote sensing.

Orbital microwave sensors can monitor daily river discharge changes.

Calibration of remote sensing signal to discharge units is necessary.

Hydrological modeling is evaluated as a method to calibrate the remote sensing.

Model-based calibration produces satisfactory results when compared to ground-based information.

Independent river discharge information can now be obtained by use of model-calibrated remote sensing.

Figure 1

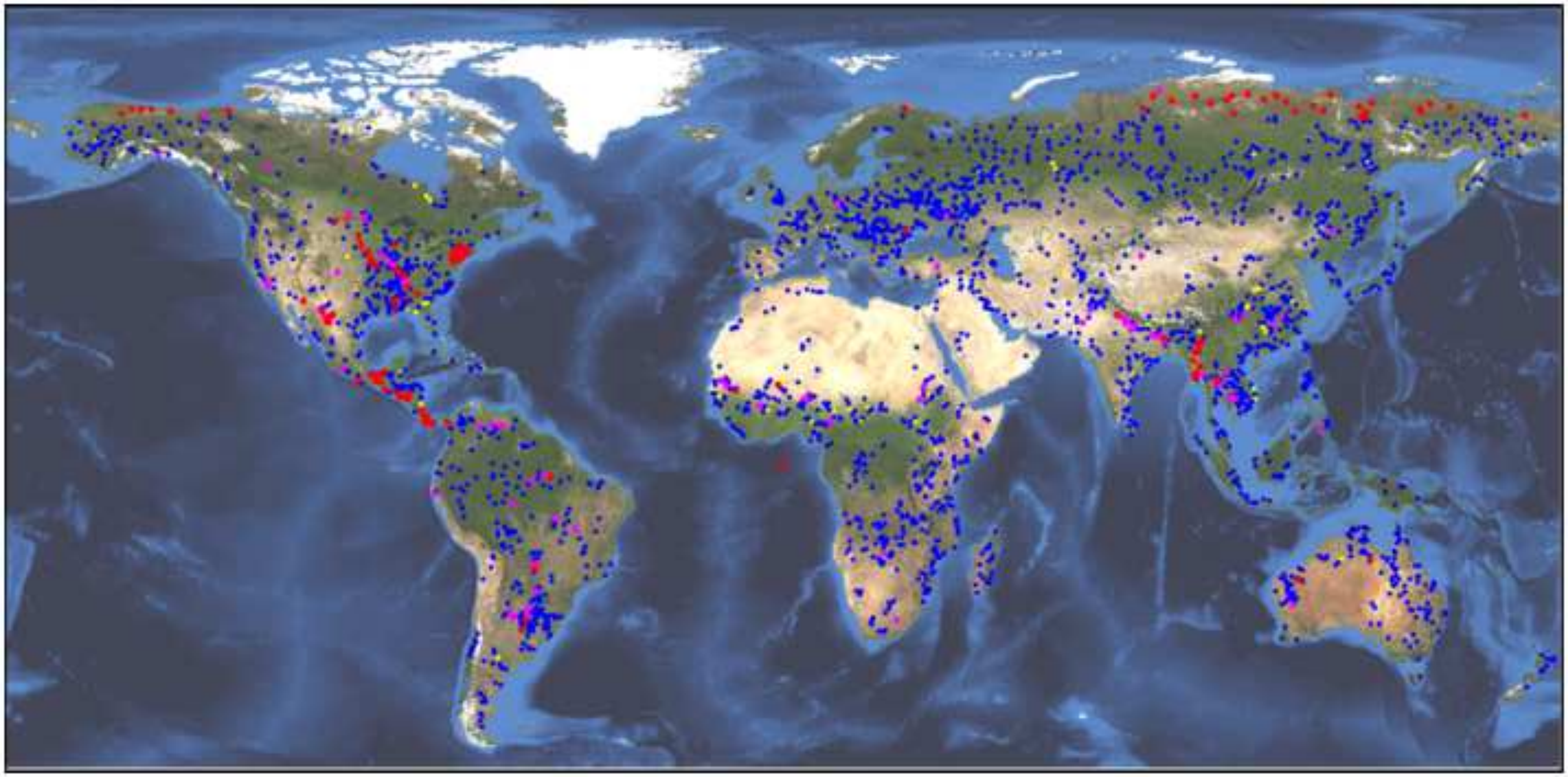

Figure 2

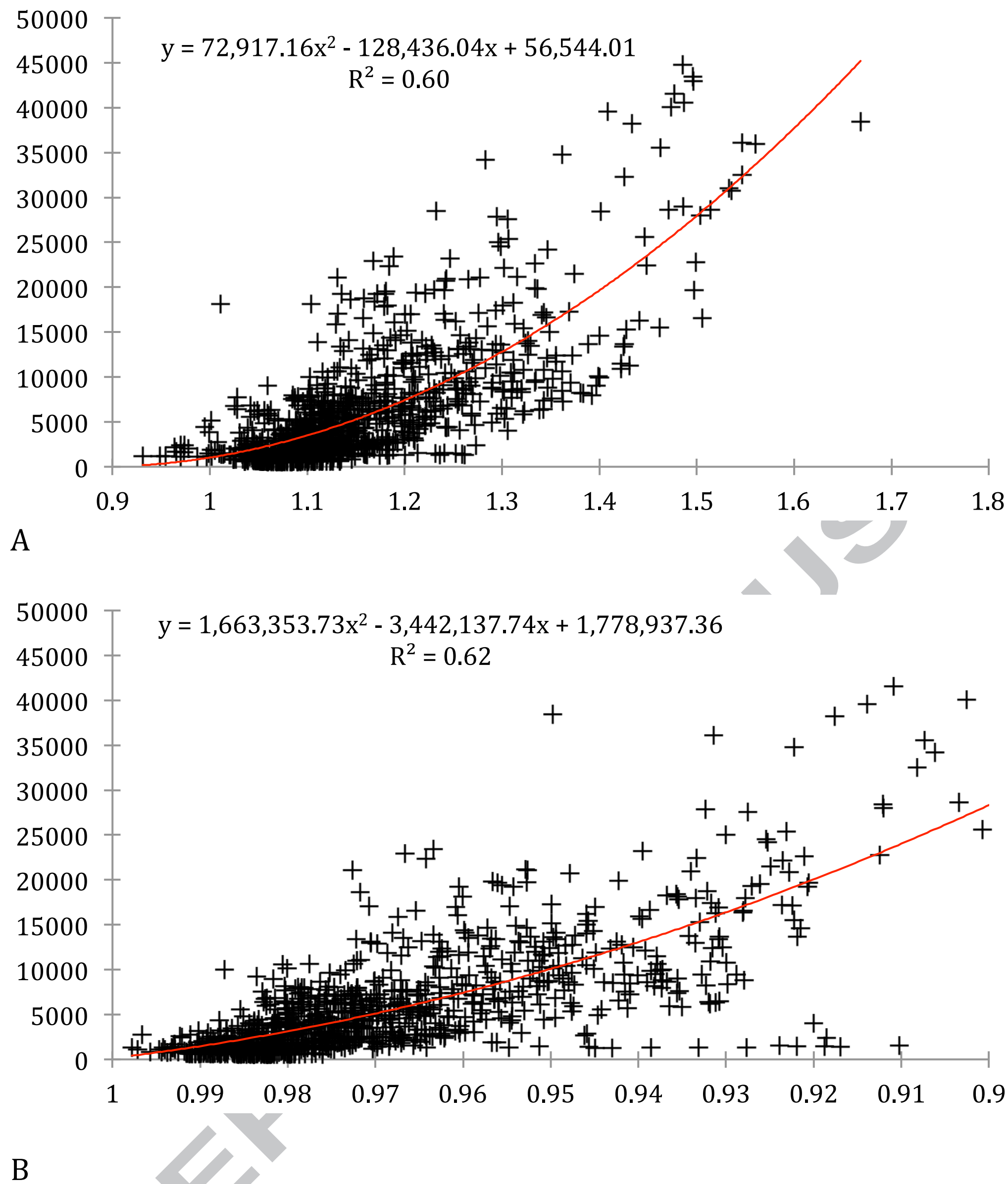
y = 72,917.16x² - 128,436.04x + 56,544.01
R² = 0.60
50000
45000
40000
35000
30000
25000
20000
15000
10000
5000
0
0.9
1
1.1
1.2
1.3
1.4
1.5
1.6
1.7
1.8
A
y = 1,663,353.73x² - 3,442,137.74x + 1,778,937.36
R² = 0.62
1
0.99
0.98
0.97
0.96
0.95
0.94
0.93
0.92
0.91
0.9
B

Figure 3

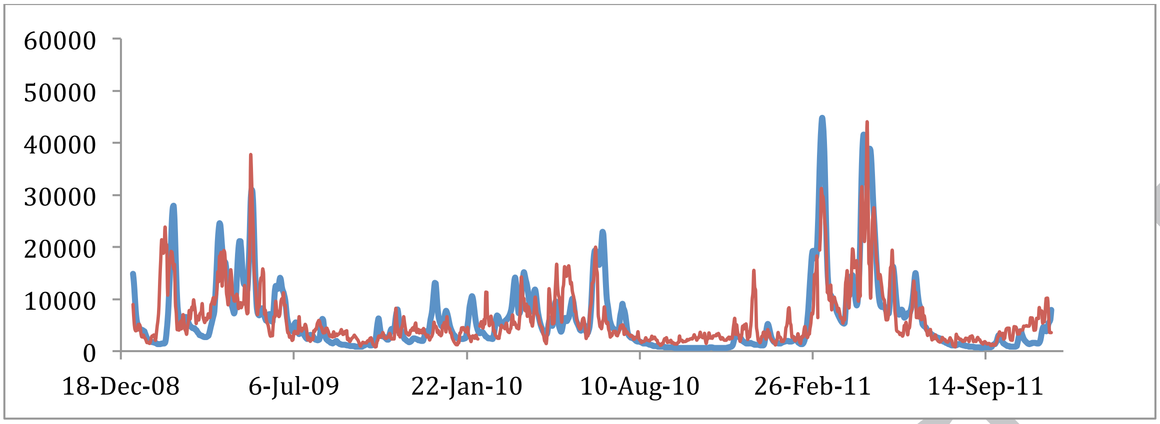
60000
50000
40000
30000
20000
10000
0
18-Dec-08
6-Jul-09
22-Jan-10
10-Aug-10
26-Feb-11
14-Sep-11

A

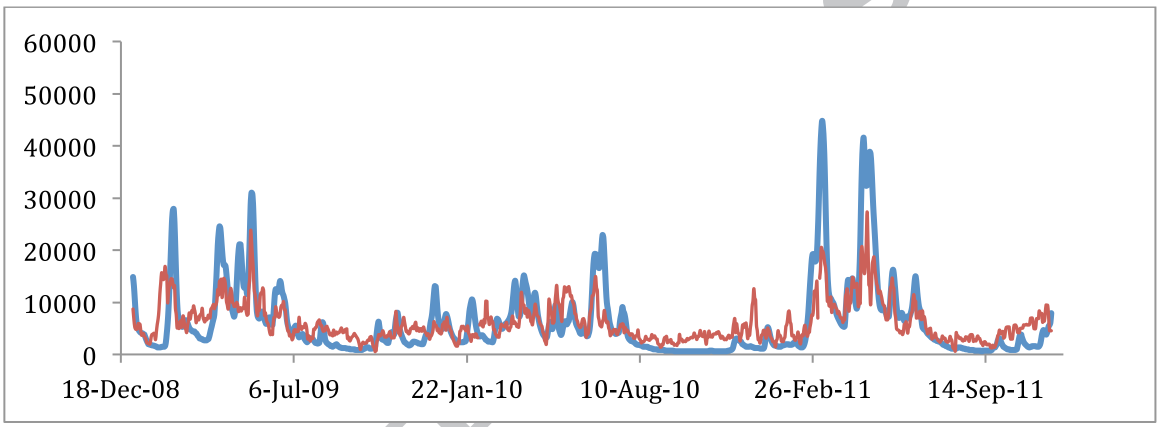
60000
50000
40000
30000
20000
10000
0
18-Dec-08
6-Jul-09
22-Jan-10
10-Aug-10
26-Feb-11
14-Sep-11

B

Figure 4

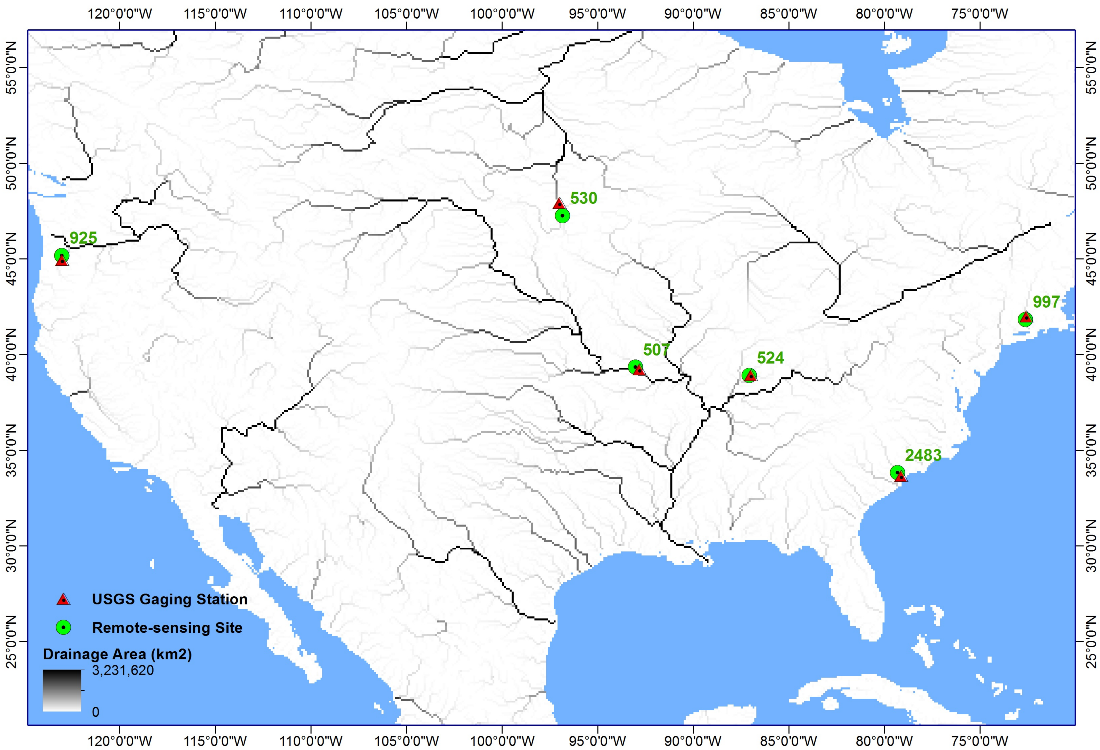

120°0'0"W
115°0'0"W
110°0'0"W
105°0'0"W
100°0'0"W
95°0'0"W
90°0'0"W
85°0'0"W
80°0'0"W
75°0'0"W
55°0'0"N
50°0'0"N
45°0'0"N
40°0'0"N
35°0'0"N
30°0'0"N
25°0'0"N
530
925
997
507
524
2483
USGS Gaging Station
Remote-sensing Site
Drainage Area (km2)
3,231,620
0

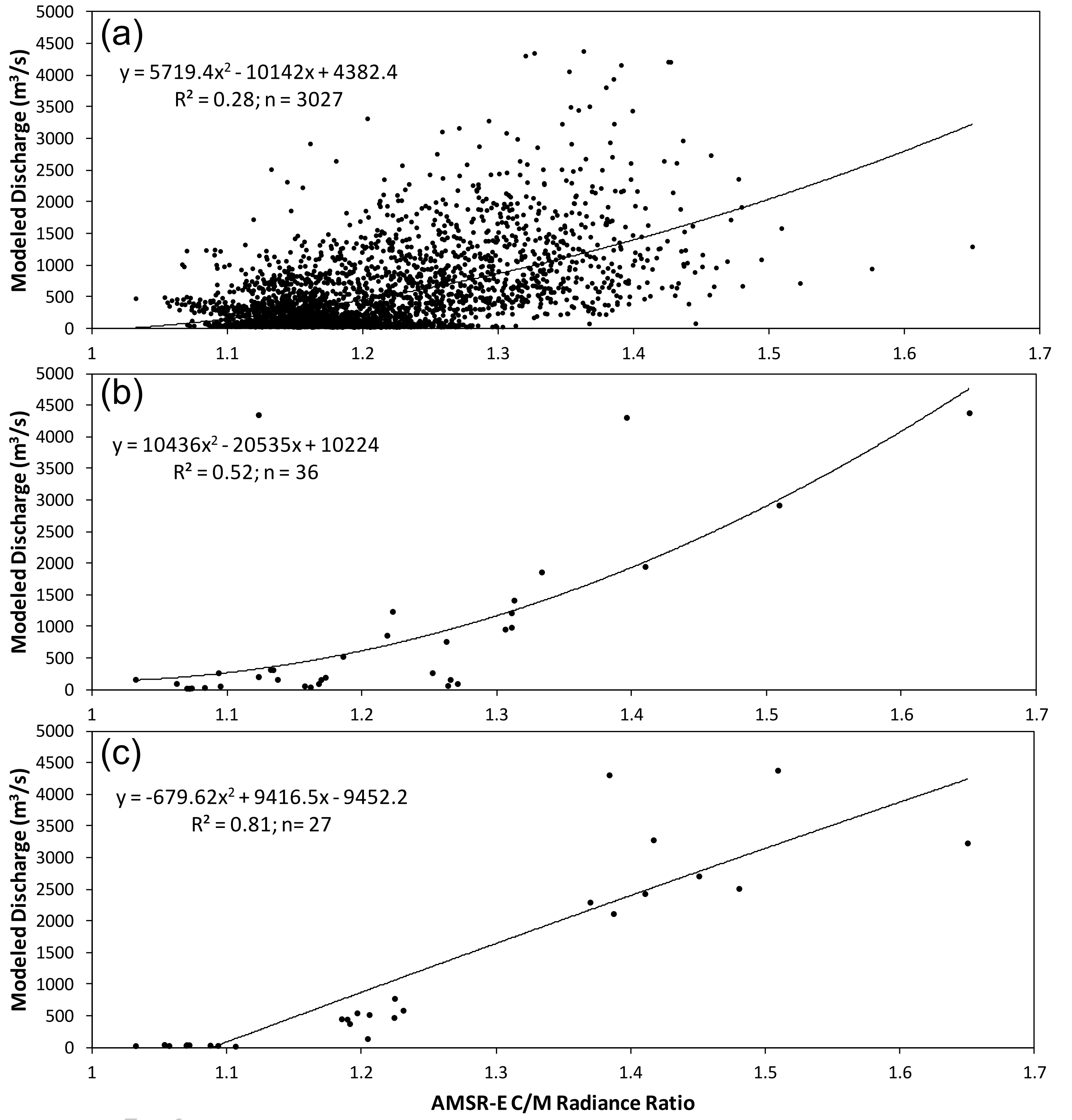

(a)
y = 5719.4x² - 10142x + 4382.4
R² = 0.28; n = 3027
(b)
y = 10436x² - 20535x + 10224
R² = 0.52; n = 36
(c)
y = -679.62x² + 9416.5x - 9452.2
R² = 0.81; n= 27
Modeled Discharge (m³/s)
AMSR-E C/M Radiance Ratio
0
500
1000
1500
2000
2500
3000
3500
4000
4500
5000
1
1.1
1.2
1.3
1.4
1.5
1.6
1.7

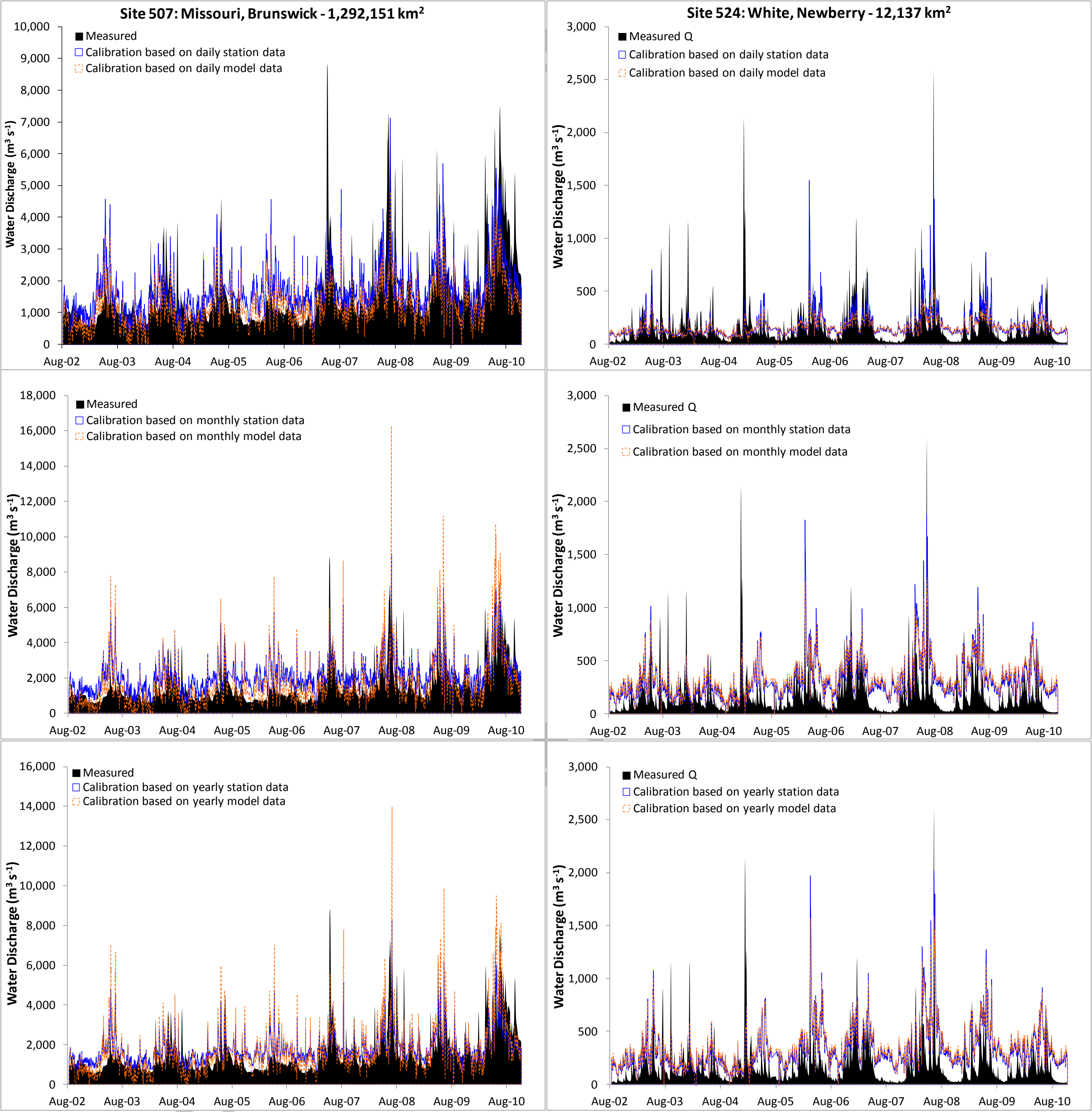

Site 507: Missouri, Brunswick - 1,292,151 km²
Site 524: White, Newberry - 12,137 km²
Measured
Measured Q
Calibration based on daily station data
Calibration based on daily model data
Calibration based on monthly station data
Calibration based on monthly model data
Calibration based on yearly station data
Calibration based on yearly model data
Water Discharge (m³ s⁻¹)
Aug-02
Aug-03
Aug-04
Aug-05
Aug-06
Aug-07
Aug-08
Aug-09
Aug-10

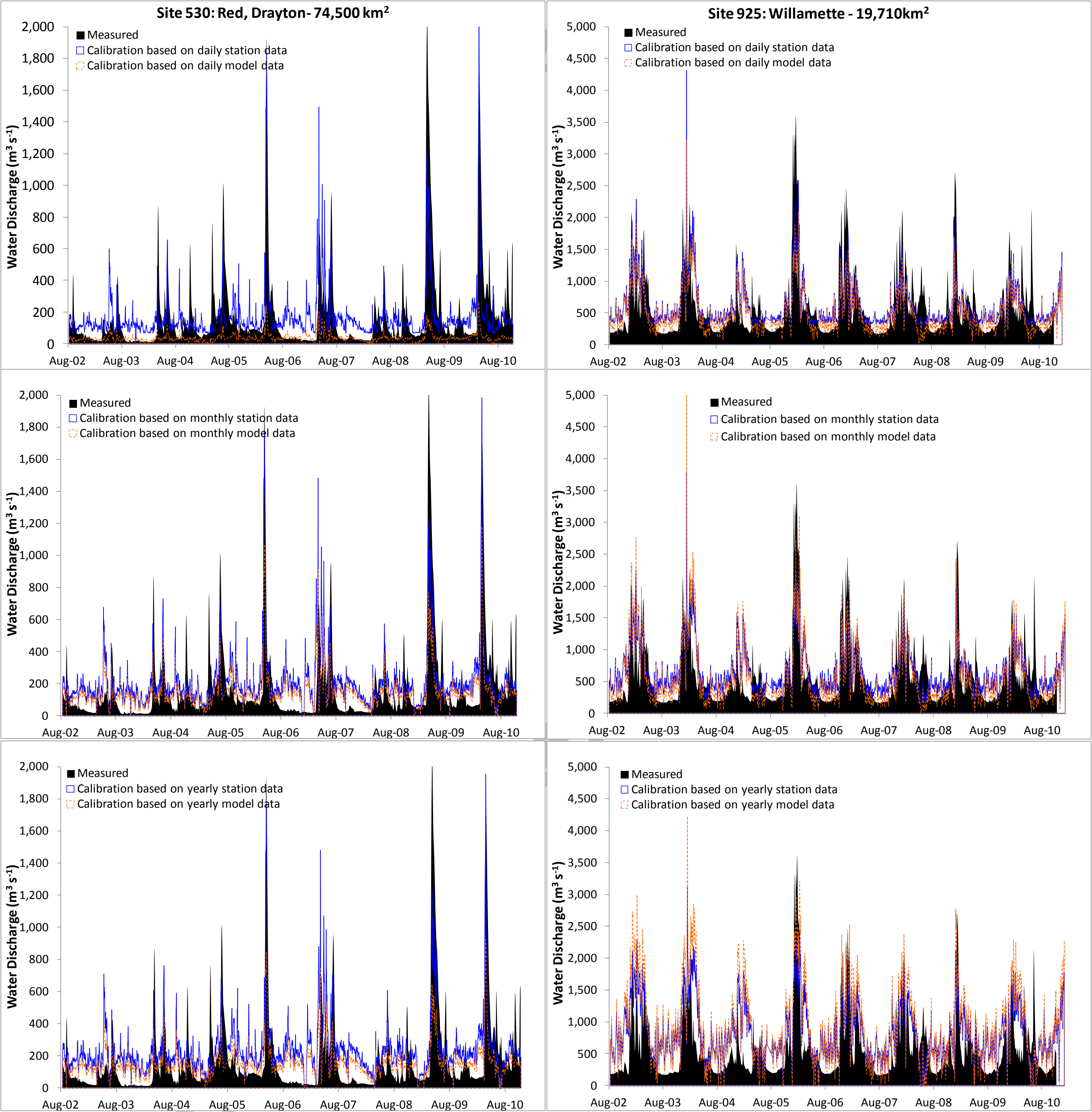

Site 530: Red, Drayton- 74,500 km2
Site 925: Willamette - 19,710km2
Measured
Calibration based on daily station data
Calibration based on daily model data
Calibration based on monthly station data
Calibration based on monthly model data
Calibration based on yearly station data
Calibration based on yearly model data
Water Discharge (m3 s-1)
0
200
400
600
800
1,000
1,200
1,400
1,600
1,800
2,000
500
1,500
2,500
3,000
3,500
4,000
4,500
5,000
Aug-02
Aug-03
Aug-04
Aug-05
Aug-06
Aug-07
Aug-08
Aug-09
Aug-10

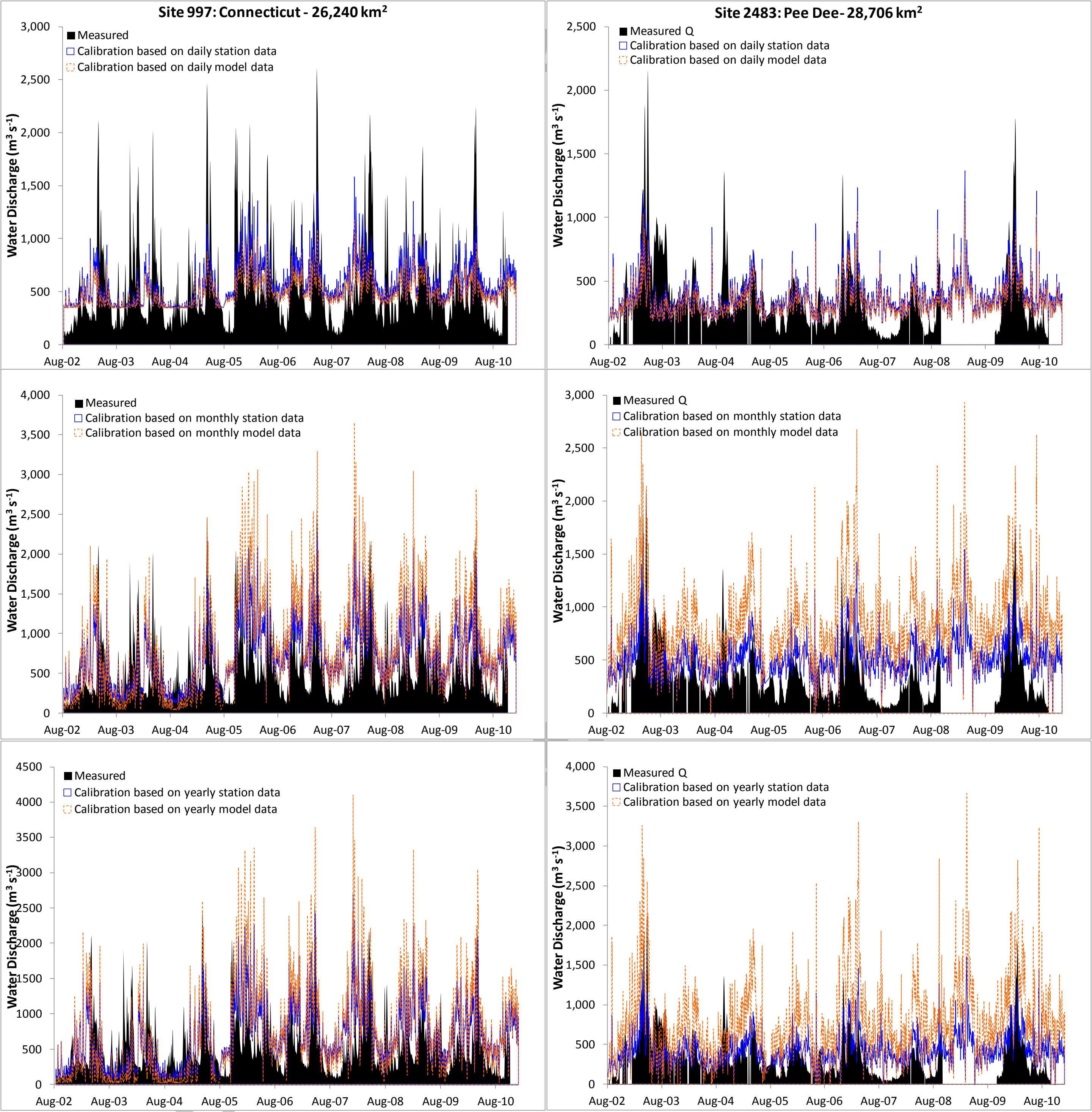
Site 997: Connecticut - 26,240 km^2
Site 2483: Pee Dee- 28,706 km^2
Measured
Calibration based on daily station data
Calibration based on daily model data
Measured Q
Calibration based on daily station data
Calibration based on daily model data
Measured
Calibration based on monthly station data
Calibration based on monthly model data
Measured Q
Calibration based on monthly station data
Calibration based on monthly model data
Measured
Calibration based on yearly station data
Calibration based on yearly model data
Measured Q
Calibration based on yearly station data
Calibration based on yearly model data
Water Discharge (m^3 s^{-1})
Aug-02
Aug-03
Aug-04
Aug-05
Aug-06
Aug-07
Aug-08
Aug-09
Aug-10

Figure 7

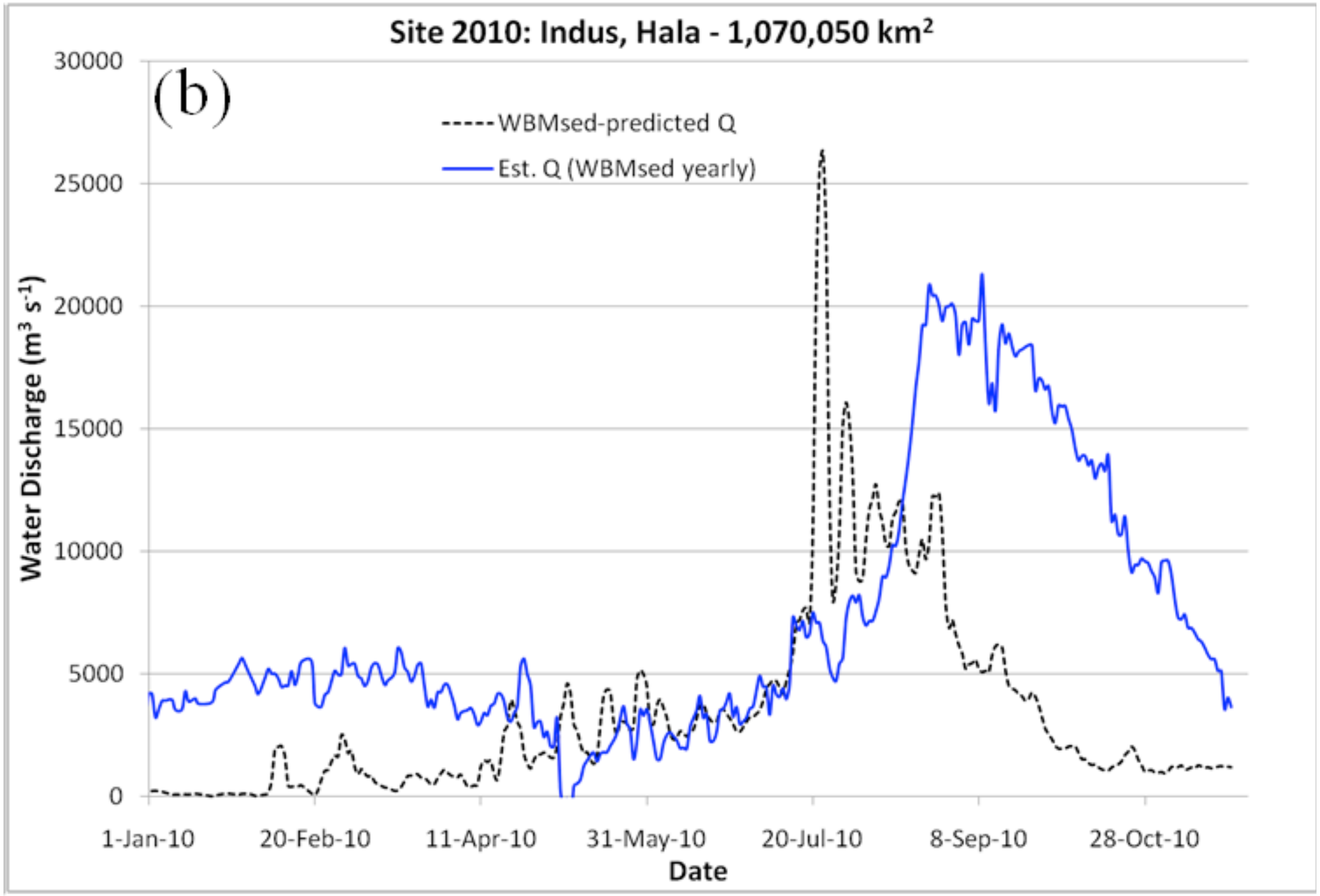

Site 2010: Indus, Hala - 1,070,050 km²
(b)
WBMsed-predicted Q
Est. Q (WBMsed yearly)
Water Discharge (m³ s⁻¹)
30000
25000
20000
15000
10000
5000
0
1-Jan-10
20-Feb-10
11-Apr-10
31-May-10
20-Jul-10
8-Sep-10
28-Oct-10
Date

Table 1. Characteristics of 6 remote-sensing sites and corresponding USGS gaging stations (Figure 1) and the Indus site and gaging station (Figure 5). Site mean discharge is as predicted by WBM.

Site ID	Site River Name	Site Coordinates Lat/Long (dd)	Site Drainage Area (km^2)	Site Mean Discharge (m^3/s)	Station ID	Station Coordinates Lat/Long (dd)	Station Drainage Area (km^2)	Station Mean Discharge (m^3/s)
507	Missouri, Brunswick	39.34/-93.02	1,264,731	1206	06906500	39.22/-92.849	1,292,151	1709
524	White, Newberry	38.91/-87.07	12,802	161	03360500	38.92/-87.011	12,137	182
530	Red, Halstad	47.26/-96.84	65,000	39	05082500	47.92/-97.029	77,929	170
925	Willamette	45.18/-123.01	19,710	504	14191000	44.94/-123.042	18,928	591
997	Connecticut	41.84/-72.632	26,240	500	01184000	41.98/-72.606	25,116	567
2483	Pee Dee	33.82/-79.32	28,706	336	02135200	33.66/-79.155	36,660	372
2010	Indus, Hala	25.9/68.26	1,070,050	2730	Mandi Plain	31.75/74.75	20,886	497

Table 2. Rating curves equations of AMSR-E C/M radiance ratios versus *WBM*-predicted and gaging station-measured discharge with daily, monthly and yearly statistics (Figure 2). Site ID corresponds to Table 1 and Figures 1 and 5.

ID	USGS daily	*WBM* daily	USGS monthly	*WBM* monthly	USGS yearly	*WBM* yearly
507	$530.71x^2 + 9092.7x - 9356.7$	$-4740.5x^2 +20231x-15676$	$1377.1x^2 +9526.3x – 10485$	$25418x^2 – 42215x + 16604$	$7548.9x^2 - 8277.2x + 1349.9$	$18291x^2 – 26997x + 8637.6$
524	$1895.9x^2 - 3321.3x + 1503.2$	$-253.99x^2 + 1280.3x - 951.57$	$-559.11x^2 + 3004.7x – 2320.3$	$935.9x^2 - 344.86x – 481.06$	$1105.2x^2 - 625.27x - 371.88$	$-22.769x^2 + 1954.5x - 1816.6$
530	$4775.2x^2 - 8733.7x + 4062.1$	$248.38x^2 - 210.5x - 11.181$	$3413.6x^2 – 5463.7x + 2180.9$	$1514.8x^2 - 1969x - + 555.27$	$3044.7x^2 - 4616.2x + 1729.7$	$665.89x^2 - 268.6x - 285.31$
925	$12268x^2 – 26478x + 14607$	$5719.4x^2 – 10142x + 4382.4$	$6893.6x^2 – 12527x + 5695.5$	$12063x^2 – 24172x + 12111$	$-996.07x^2 + 7989.8x - 7354.3$	$-679.62x^2 + 9416.5x - 9452.2$
997	$17051x^2 – 34488x + 17789$	$10897x^2 – 21890x + 11338$	$22195x^2 – 42451x + 20421$	$40085x^2 – 78585x + 38557$	$29201x^2 – 57348x + 28248$	$57460x^2 – 116560x + 59142$
2483	$21959x^2 – 41141x + 19441$	$17858x^2 – 33431x + 15821$	$17411x^2 – 29828x + 12726$	$38582x^2 – 67080x + 28870$	$18563x^2 – 32388x+ 14093$	$46022x^2 – 80588x + 34948$